AMERICAN SOCIETY FOR MICROBIOLOGY | Antimicrobial Agents and Chemotherapy®

CLINICAL THERAPEUTICS

In Vivo Bioluminescent Monitoring of Therapeutic Efficacy and Pharmacodynamic Target Assessment of Antofloxacin against *Escherichia coli* in a Neutropenic Murine Thigh Infection Model

Yu-Feng Zhou,[a,b] Meng-Ting Tao,[a,b] Yu-Zhang He,[a,b] Jian Sun,[a,b] Ya-Hong Liu,[a,b] Xiao-Ping Liao[a,b]

[a]National Risk Assessment Laboratory for Antimicrobial Resistance of Animal Original Bacteria, South China Agricultural University, Guangzhou, China

[b]Guangdong Provincial Key Laboratory of Veterinary Pharmaceutics Development and Safety Evaluation, South China Agricultural University, Guangzhou, China

ABSTRACT Antimicrobial resistance among uropathogens has increased the rates of infection-related morbidity and mortality. Antofloxacin is a novel fluoroquinolone with broad-spectrum antibacterial activity against urinary Gram-negative bacilli, such as *Escherichia coli*. This study monitored the *in vivo* efficacy of antofloxacin using bioluminescent imaging and determined pharmacokinetic (PK)/pharmacodynamic (PD) targets against *E. coli* isolates in a neutropenic murine thigh infection model. The PK properties were determined after subcutaneous administration of antofloxacin at 2.5, 10, 40, and 160 mg/kg of body weight. Following thigh infection, the mice were treated with 2-fold-increasing doses of antofloxacin from 2.5 to 80 mg/kg administered every 12 h. Efficacy was assessed by quantitative determination of the bacterial burdens in thigh homogenates and was compared with the bioluminescent density. Antofloxacin demonstrated both static and killing endpoints in relation to the initial burden against all study strains. The PK/PD index area under the concentration-time curve (AUC)/MIC correlated well with efficacy ($R^2 = 0.92$), and the dose-response relationship was relatively steep, as observed with escalating doses of antofloxacin. The mean free drug AUC/MIC targets necessary to produce net bacterial stasis and 1-$\log_{10}$ and 2-$\log_{10}$ kill for each isolate were 38.7, 66.1, and 147.0 h, respectively. *In vivo* bioluminescent imaging showed a rapid decrease in the bioluminescent density at free drug AUC/MIC exposures that exceeded the stasis targets. The integration of these PD targets combined with the results of PK studies with humans will be useful in setting optimal dosing regimens for the treatment of urinary tract infections due to *E. coli*.

KEYWORDS antofloxacin, bioluminescence, PK/PD, murine thigh infection, *Escherichia coli*

Acute pyelonephritis (AP) is a serious urinary tract infection with symptoms that range from a slight indisposition to life-threatening illness and even death (1). In the United States, at least 250,000 episodes of AP occur each year, mostly among women, resulting in over $2 billion in health care costs annually (2, 3). More than 85% of AP cases are bacterial infections, and the members of the family *Enterobacteriaceae*, especially *Escherichia coli*, are the causative agents (4). However, the antimicrobial susceptibility patterns of *E. coli* isolates causing AP vary considerably in different regions and countries (5, 6). The Infectious Diseases Society of America (IDSA) recommended fluoroquinolones as the initial empirical therapy for AP patients in area where the prevalence of resistance of community uropathogens to trimethoprim-sulfamethoxazole exceeds 20% and that to fluoroquinolones is less than 10% (7). However, the incidence of quinolone-resistant uropathogens has increased significantly

Received 21 June 2017 **Returned for modification** 30 July 2017 **Accepted** 16 September 2017

Accepted manuscript posted online 16 October 2017

Citation Zhou Y-F, Tao M-T, He Y-Z, Sun J, Liu Y-H, Liao X-P. 2018. *In vivo* bioluminescent monitoring of therapeutic efficacy and pharmacodynamic target assessment of antofloxacin against *Escherichia coli* in a neutropenic murine thigh infection model. Antimicrob Agents Chemother 62:e01281-17. https://doi.org/10.1128/AAC.01281-17.

Address correspondence to Xiao-Ping Liao, xpliao@scau.edu.cn.

TABLE 1 Antofloxacin dose and *f*AUC/MIC needed to achieve various degrees of antibacterial effects *in vivo* for each *E. coli* isolate[a]

E. coli isolate	MIC (mg/liter)	Burden at start of therapy (log_{10} no. of CFU/thigh)	*In vivo* fitness[b]	$fAUC_{24}$/MIC of antofloxacin (h) needed to achieve:			24-h total dose of antofloxacin (mg/kg) needed to achieve:		
				Net static	1-log kill	2-log kill	Net static	1-log kill	2-log kill
160179	0.063	5.96	1.83	43.1	91.7	153	5.92	15.3	32.6
161406	0.125	6.33	1.68	57.1	87.8	155	12.2	22.8	50.7
161549	0.125	6.19	1.91	58.4	94.1	168	12.3	25.4	55.3
ATCC 25922	0.25	6.39	1.84	32.2	50.6	NA	14.8	29.2	NA
161673	0.5	6.31	1.38	42.3	71.1	112	51.5	94.1	151
16X109	0.5	6.18	2.12	35.4	58.9	NA	42.1	77.3	NA
16X327	1	6.09	1.71	28.1	47.4	NA	71.7	127	NA
161666	2	6.03	1.98	13.3	27.9	NA	63.7	138	NA
Mean		6.19	1.81	38.7	66.1	147	34.3	66.1	72.4
SD		0.14	0.21	13.9	22.4	20.8	24.4	46.5	46.1

[a]*f*AUC, AUC for the unbound fraction (not protein bound); NA, not achieved.
[b]Defined as the growth (log_{10} number of CFU per thigh) of the bacterial isolate in untreated mice.

in recent years (8). Fluoroquinolones are therefore considered the preferred option for treating urinary tract infections due to susceptible *E. coli* strains (9). In addition, there is evidence that ciprofloxacin may be an appropriate choice for empirical therapy of uncomplicated AP in areas with high rates of ciprofloxacin resistance, if it is tailored appropriately on the basis of susceptibility data (10). More importantly, therapeutic efficacy is under the control of rational dosing regimens that ensure a high probability of clinical and microbiological success. These investigations into pharmacodynamic targets have been critical for defining the optimal antimicrobial exposure as a measure of *in vivo* potency (11).

Antofloxacin is a novel levofloxacin derivative approved by the China Food and Drug Administration (CFDA) for the treatment of acute uncomplicated cystitis and AP due to *E. coli* (12). This drug targets the urinary tract, judging from the high urine drug concentrations (13). The results of urine antofloxacin assays indicated that 40 to 45% of the parent drug is excreted in the urine by 72 h after administration (14). An oral formulation of antofloxacin with promising pharmacokinetic and efficacy results has been developed. Antofloxacin showed linear pharmacokinetic characteristics with a mean half-life of 20.3 h in healthy volunteers (14), which was significantly longer than that of other fluoroquinolones, such as ciprofloxacin, levofloxacin, and gatifloxacin (15, 16). Previous clinical studies in patients with acute exacerbations of chronic bronchitis (AECB) and AP have demonstrated the potency and efficacy of antofloxacin against *Staphylococcus aureus*, *Streptococcus pneumoniae*, and *Haemophilus influenzae* as well as members of the family *Enterobacteriaceae*, especially *E. coli* (17). However, a definitive determination of the optimal antofloxacin exposure and the impact of variations in MICs remain unclear. The goals of this study were to determine pharmacokinetic (PK)/pharmacodynamic (PD) target values for antofloxacin against urinary *E. coli* isolates with various MICs using exposure-response modeling. We wanted to monitor the *in vivo* efficacy of antofloxacin using the quantitative bacterial burdens and *in vivo* bioluminescent imaging (BLI) in a neutropenic murine thigh infection model. We propose that the integration of these PD targets with human pharmacokinetic data may provide a rational framework for the design of optimal dosing regimens for the treatment of AP due to *E. coli*.

RESULTS

Organism susceptibility and *in vivo* fitness. The MICs of antofloxacin against the *E. coli* isolates tested varied from 0.063 to 2 mg/liter. At the start of therapy, mice had 6.19 ± 0.14 log_{10} CFU/thigh, and the infectious burden in untreated control mice increased to 8.00 ± 0.21 log_{10} CFU/thigh after 24 h. The organisms showed similar levels of *in vivo* fitness, with bacterial growth being 1.38- to 2.12-log_{10} CFU in the thigh homogenates of untreated mice (Table 1). Among eight *E. coli* isolates available, only

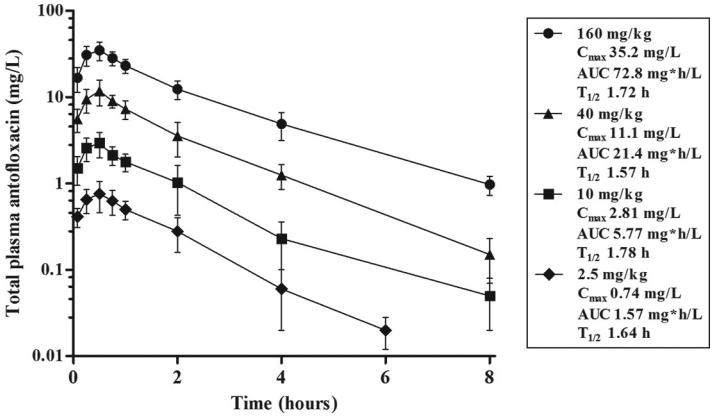

FIG 1 Plasma drug concentrations after administration of single subcutaneous doses of antofloxacin in infected neutropenic mice. Error bars represent the standard deviations of the concentrations measured in six mice. Pharmacokinetic parameters listed in the box include the peak (maximum) concentration (C_{max}) in plasma, the AUC from time zero to infinity (AUC), and the elimination half-life ($t_{1/2}$) for each dose.

two strains harbored *qnrS* (see Table S1 in the supplemental material). However, these strains had low MICs of less than 1 mg/liter. None of the isolates had a mutation in *gyrA* or *parC*, but one isolate harbored $bla_{CTX\text{-}M\text{-}1G}$.

Drug pharmacokinetics. The time course of the antofloxacin concentrations in plasma was best fitted by a one-compartment model with first-order absorption. The elimination half-life ($t_{1/2}$) ranged from 1.57 to 1.78 h. Over the dose range of 2.5 to 160 mg/kg of body weight, the pharmacokinetics followed a linear pattern ($R^2 > 0.99$) in a dose-dependent manner. Peak concentrations ranged from 0.74 to 35.2 mg/liter. The values of the area under the concentration-time curve (AUC) from time zero to infinity ($AUC_{0-\infty}$) ranged from 1.57 to 72.8 mg · h/liter (Fig. 1).

Dose-response relationships. Antofloxacin was quite potent against our *E. coli* isolates over the dose range studied. The dose-response curves were steep, with a 2-fold increase in drug exposure producing a 1- to 2-$\log_{10}$ change in the antimicrobial effect. In comparison to the initial burden, a 1-$\log_{10}$ kill against all strains was observed and a 2-$\log_{10}$ or greater kill against four of eight strains was achieved. The maximal effect from the start of therapy was almost a 3-$\log_{10}$ kill for two of the strains (strains 160179 and 161549) (Fig. 2). The higher dosages were necessary to achieve similar outcomes against *E. coli* isolates with elevated antofloxacin MICs.

Pharmacodynamic index and target. The relationship between the organism burden in the thighs and the plasma free drug AUC (*f*AUC)/MIC ratio was fit to the sigmoidal maximum-effect (E_{max}) model. On the basis of regression analysis, the PK/PD index AUC/MIC was a robust predictor of efficacy against all *E. coli* isolates studied ($R^2 = 0.92$) (Fig. 3). The free drug AUC/MIC ratio associated with a net static effect and 1-$\log_{10}$ kill ranged from 13.3 to 58.4 h and 27.9 to 94.1 h, respectively. The mean AUC/MIC target for 2-$\log_{10}$ kill was roughly 2-fold greater than that associated with the 1-$\log_{10}$ kill endpoint (147 h versus 66.1 h). In addition, the total daily doses needed to produce a bacteriostatic effect and 1-$\log_{10}$ and 2-$\log_{10}$ kill (when achieved) were 34.3, 66.1, and 72.4 mg/kg, respectively (Table 1).

Bioluminescent plasmid stability and strain characterizations. A kinetic *in vivo* study of mice infected with *E. coli* 161549/pAK*lux*2 was performed to determine the bioluminescent plasmid stability during thigh infections. Measurements taken over the course of the infections showed no statistically significant differences ($P > 0.36$) in the bacterial counts on the plates in the presence or absence of ampicillin (Fig. 4A). This indicated that pAK*lux*2 was stable in *E. coli in vivo* up to 48 h postinfection. Additionally, to determine if the bioluminescent plasmid altered the virulence of *E. coli in vivo*, we compared the growth kinetics of *E. coli* 161549 with and without the plasmid. Both

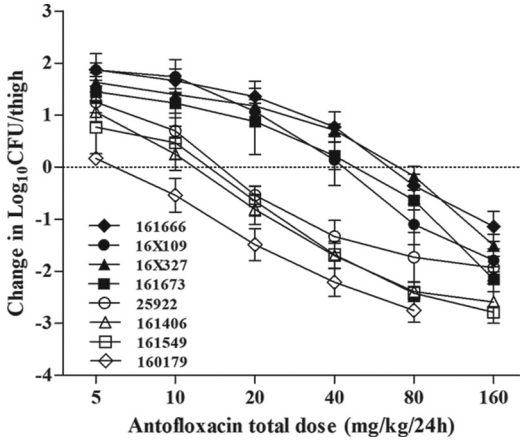

FIG 2 *In vivo* dose-response curves for antofloxacin against *E. coli* using a neutropenic murine thigh infection model. Mice received one of a series of 2-fold increasing doses of antofloxacin every 12 h over a 24-h treatment period. Each symbol represents the mean organism burden for four thighs. The horizontal dashed line represents the net stasis of the burden from the start of therapy. Data points below the line represent bactericidal activity, and points above the line represent net growth.

groups of mice exhibited the same patterns of bacterial burdens throughout the study time. The bacterial counts in thighs from mice infected with *E. coli* 161549 containing the plasmid were numerically lower than those in thighs from mice infected with *E. coli* 161549 without the plasmid, but the difference was not statistically significant ($P > 0.14$) (Fig. 4B). The slight growth delay, which resulted in a delay in the progression of infection, caused by bioluminescent plasmid pAK*lux*2 did not significantly alter the virulence of the strain. This finding supports the feasibility of using bioluminescence as a quantitative indicator of *E. coli* thigh infection *in vivo*.

***In vivo* bioluminescent monitoring of therapeutic efficacy.** The therapeutic efficacy of antofloxacin was monitored continuously using bioluminescent imaging (BLI) of *E. coli* 161549/pAK*lux*2 in mice at 2 h postinoculation. In untreated mice, the spread of bioluminescence and intensity increased considerably with inocula of both 10^6 and 10^8 CFU/thigh (Fig. 5A). The radiance intensity reached a maximum at 48 h, at which time all untreated mice showed pronounced symptoms of disease (Fig. 5B).

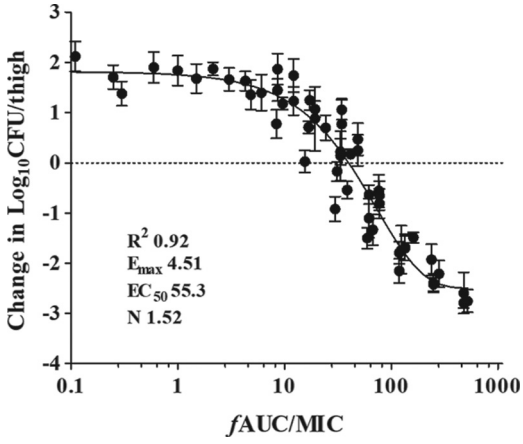

FIG 3 Relationship between the antofloxacin plasma 24-h *f*AUC/MIC ratios and the *in vivo* microbiological effect against multiple isolates of *E. coli*. Each symbol represents the mean organism burden for four thighs. Each of six drug dose levels was fractionated into a regimen administered every 12 h. The horizontal dashed line represents the net stasis of the burden from the start of therapy. Data points below the line represent killing, and points above the line represent growth. The line drawn through the data points is the best-fit line based upon the sigmoidal E_{max} formula.

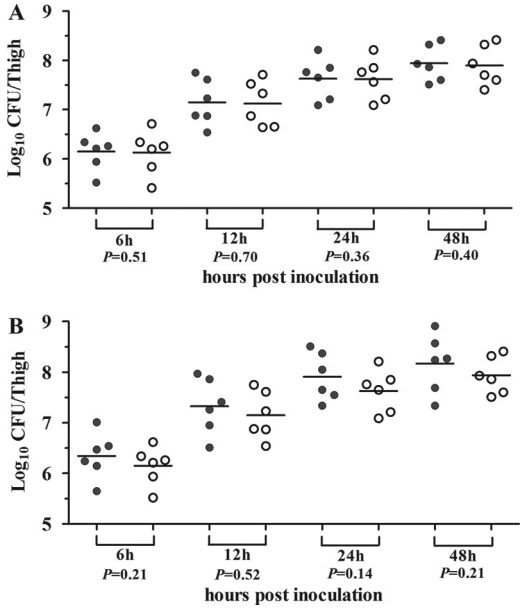

FIG 4 (A) Bacterial loads in mice infected with *E. coli* 161549 containing pAK*lux*2 plated on MHA alone (gray circles) and MHA with ampicillin (white circles). (B) Bacterial loads in mice infected with wild-type *E. coli* 161549 (gray circles) or *E. coli* 161549 carrying pAK*lux*2 (white circles). Each point represents a value from a single thigh, and the horizontal lines represent the mean for the group. Animals were infected with ~10^6 CFU of bacteria in each posterior thigh. Tissues were homogenized and plated for determination of bacterial counts at the indicated time points.

However, bioluminescence in mice treated with antofloxacin showed a progressive reduction. With the low inoculum, antofloxacin therapy produced densities of both radiance and the organism burden in thighs significantly lower than those observed with the high inoculum ($P < 0.01$). After 48 h of treatment, antofloxacin could achieve 3.93-$\log_{10}$ and 3.72-$\log_{10}$ killing of bacteria compared to the initial burdens achieved with the inocula of 10^6 and 10^8 CFU/thigh, respectively (Fig. 5C). There was no significant relapse after the discontinuation of drug therapy (data not shown).

There was an excellent correlation between the bacterial burdens and bioluminescence *in vitro* and within the host tissues, where the R^2 values for culture media and thigh tissues were 0.97 and 0.93, respectively (Fig. S1). When the bioluminescent data were fit to a sigmoidal E_{max} model, the free drug AUC/MIC (*f*AUC/MIC) ratios and radiance values showed a strong correlation ($R^2 = 0.83$) (Fig. S2), although it was less than that achieved with the microbiological endpoint ($R^2 = 0.92$) (Fig. 3). In addition, the PD targets calculated on the basis of the bioluminescent endpoints were similar to the targets traditionally used for *E. coli* 161549 (Table S2), indicating that bioluminescence may be employed to estimate PD targets at specific sites of infection without animal sacrifice.

DISCUSSION

The present study demonstrated the *in vivo* therapeutic efficacy and PK/PD relationships of antofloxacin against urinary *E. coli* isolates displaying a wide range of MICs. This potent activity has been observed *in vitro* and *in vivo* against both *S. aureus* and *Mycobacterium tuberculosis* (18, 19). Our previous studies with antofloxacin showed a dose-dependent activity with prolonged postantibiotic effects against *Klebsiella pneumoniae* in a model of lung infection in neutropenic mice (20). Similar to other fluoroquinolones, the most predictive PK/PD index of antofloxacin associated with efficacy against *E. coli* was the free drug AUC/MIC (21, 22). This index provided a useful measure of exposure for data modeling using a sigmoidal E_{max} model. We established that the PD target required to achieve a 1-$\log_{10}$ kill effect was 66.1 h for *E. coli*, which was 2-fold lower than that generally quoted for fluoroquinolones against Gram-negative bacilli of

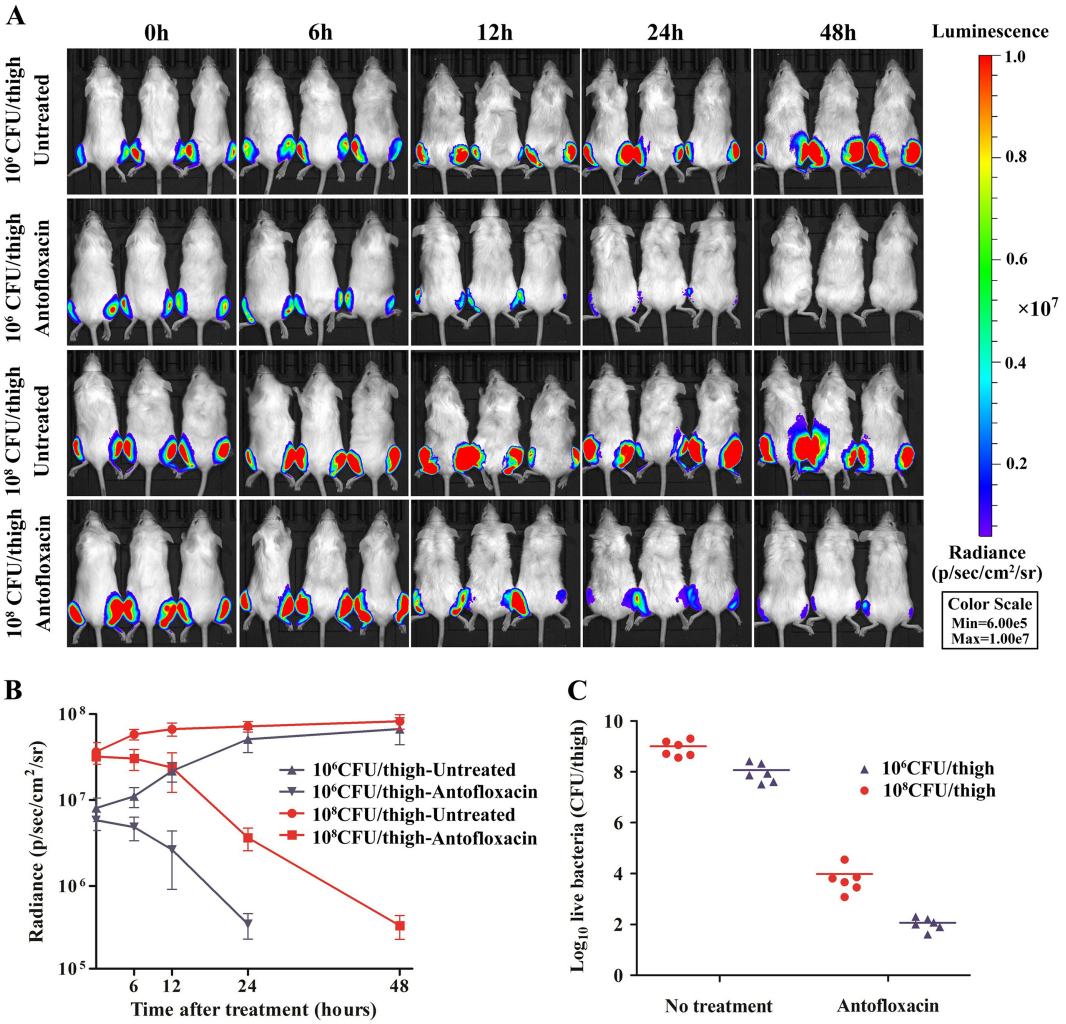

FIG 5 Monitoring of the therapeutic efficacy of antofloxacin in a murine thigh infection model by use of *in vivo* bioluminescent imaging data. (A) Bioluminescence in mice infected with *E. coli* 161549 containing pAK*lux*2 at 10^6 or 10^8 CFU/thigh. Mice were administered antofloxacin at 20 mg/kg subcutaneously every 12 h for 2 days. Images were taken at 2 h after thigh infection (0 h) and then at 6, 12, 24, and 48 h after treatment. Mice were anesthetized with isoflurane during imaging procedures. Bioluminescence is reported as radiance (number of photons per second per square centimeter per steradian [p/sec/cm²/sr]) on a scale paired with a color bar shown next to the images. (B) Quantification of time course-dependent bioluminescent imaging data in mice. Data are expressed as the mean ± standard deviation (SD). (C) Comparison of the bacterial burdens in the untreated control and antofloxacin treatment groups. Bacterial visible counts were conducted 48 h after treatment. Antofloxacin produced 3.93-$\log_{10}$ and 3.72-$\log_{10}$ reductions compared to the initial burdens achieved with 10^6 and 10^8 CFU/thigh, respectively.

100 to 125 h (23). Specifically, antofloxacin exhibited a classical sigmoidal exposure-response relationship with the *E. coli* isolates used in this study. The curve shape was steep, and relatively small increases in drug exposure resulted in large increases in antimicrobial effects. Although it is currently unclear how the shape of this curve relates to clinical efficacy, the pharmacodynamic targets of antofloxacin exceeding both the static and 1-$\log_{10}$ kill for these urinary *E. coli* isolates could be utilized for the prediction of efficacy in humans. Consistent with this view, a previous phase II clinical study conducted in 143 cases of AP indicated that antofloxacin and levofloxacin have comparable bacteriological efficacies (95.9% versus 92.4%, respectively) (17).

Bioluminescent imaging (BLI) provides a method that allows the visualization of bacterial viability in host tissues and better monitoring of therapeutic efficacy *in vivo*. The noninvasive real-time BLI method has been developed and validated for application to quantitative antimicrobial treatment in the neutropenic murine thigh infection

model in which the infection is due to bioluminescent *E. coli*, potentially with an improved limit of detection (24). Despite the limitation of genetic manipulation for clinical isolates, many bioluminescent model pathogens, such as *E. coli* Xen 14, *S. aureus* Xen 30, and *S. pneumoniae* Xen 10, could be employed to noninvasively monitor therapeutic efficacy (25–27). In this study, we demonstrated that the pAK*lux*2 plasmid had no effect on the virulence of clinical *E. coli* strains, which makes it an excellent biosensor suitable for conducting therapeutic studies *in vivo*. More importantly, the bioluminescent densities were closely related to the quantitative burdens of *E. coli* in the thighs over the range of concentrations used for treatment (see Fig. S1 and S2 in the supplemental material), showing the feasibility of the use of bioluminescence as an alternative approach to estimate PD targets. There are many advantages to the use of BLI in PK/PD research (28, 29), including the following: (i) minimization of the number of animals used to perform time course studies by eliminating animal sacrifices at specific time points to enumerate bacterial burdens, (ii) eradication of the requirement for additional steps to estimate bacterial numbers in target tissues, reducing the processing time and cost, (iii) reduction of individual variations, since bacterial viability is monitored in the same group of animals over the study period, and (iv) identification of bacterial dissemination to unexpected host tissues. In addition, the use of bioluminescent bacteria allows the earlier prediction of therapeutic efficacy.

The incidence of fluoroquinolone resistance among urinary *E. coli* isolates associated with bacteriologic and clinical failure in patients has been increasing (30). However, it remains a common practice to prescribe fluoroquinolones, such as levofloxacin, norfloxacin, and ciprofloxacin, for the treatment of urinary tract infections (9). Indeed, *in vitro* resistance would not be expected to predict the clinical outcomes of urinary tract infections since urine antimicrobial levels are generally significantly higher than serum levels for most fluoroquinolones (13, 15). For cystitis, the microbiological endpoints can frequently be achieved, despite the *in vitro* resistance of the uropathogens to fluoroquinolones (31). Acute pyelonephritis is considered a deep-tissue infection for which adequate drug exposure in serum is important (32).

Experimental PK/PD analyses are useful for predicting clinical treatment outcomes (33). Administration of a single 400-mg dose of antofloxacin orally to healthy human volunteers resulted in a mean free drug AUC of 55 mg · h/liter, suggesting 17.5% plasma protein binding in humans (12, 14). If the loading dose of 400 mg is given orally, antofloxacin is estimated to be effective against isolates with MICs of up to 1 mg/liter, while it achieves an *f*AUC/MIC of $>$55 h, which was close to the highest static target (58.4 h) identified herein for *E. coli* strains. Likewise, the phase II clinical dose-finding study using a population PK model found that the 400-mg loading dose with a maintenance dose of 200 mg/day was associated with AUC/MIC targets of $>$20 h against *E. coli* strains with MICs of 1 mg/liter (34). This result was congruent with the corresponding static target of 28.1 h for *E. coli* strains having a MIC of 1 mg/liter identified in this study. The susceptibility breakpoint for antofloxacin remains unclear. In 2016, surveillance antimicrobial susceptibility results in the National Risk Assessment Laboratory for Antimicrobial Resistance of Animal Original Bacteria for antofloxacin against urinary *E. coli* (64 strains) demonstrated an MIC_{90} of 2 mg/liter, with a range of 0.015 to 8 mg/liter (Fig. S3). On the basis of the results of AUC exposures in humans, the current PD targets, and the MIC distribution in this study, a 10,000-subject Monte Carlo simulation (Oracle Crystal Ball software) indicated that the probabilities of target attainment (PTA) could reach 85.7% and 90.6% when antofloxacin was administered at oral doses of 200 and 400 mg/day, respectively (Fig. S4). These findings would be beneficial in optimizing clinical dosing regimens for AP and setting preliminary susceptibility breakpoints for antofloxacin. In addition, the results of previous clinical trials of treatments for adult AP showed that a loading dose of 400 mg antofloxacin followed by 200 mg daily resulted in a 93.7% cure rate, whereas the administration of 200 mg levofloxacin twice daily (the approved regimen in China) was associated with an 89.8% cure rate (17).

The well-established neutropenic murine thigh infection model has been widely

employed to determine the exposure-response relationships for diverse antimicrobials, including antofloxacin and other fluoroquinolones (18, 22). The magnitudes of the AUC/MIC ratios required for the efficacy of antofloxacin against *E. coli* in the neutropenic murine thigh infection model were similar to those for gatifloxacin and garenoxacin (22, 35) but greater than those for some novel bacterial type II topoisomerase inhibitors (NBTI) (36, 37). The relatively elevated PD targets may be due to the presence of neutrophils in the thigh infection model. Consistent with this view, the previous studies with gatifloxacin in a thigh infection model indicated that the AUC/MIC targets for efficacy were more than 2-fold greater than those in the nonneutropenic model (22). In addition, the use of a thigh infection model may limit the applicability of our results to urinary tract disease. However, in a recent study with a novel NBTI, 5463, the efficacies against *E. coli* strains in mouse models of lung, thigh, and ascending urinary tract infections were observed to be similar (38).

Fluoroquinolones containing a methyl or amino substitution may, in theory, induce QTc prolongation and arrhythmias (39). However, examinations of the toxicity of five daily injections of antofloxacin in beagle dogs showed that a QTc prolongation did not occur at doses of 10, 20, and 40 mg/kg (17). Similarly, in healthy male volunteers, multiple doses of antofloxacin ranging from 50 to 500 mg were well tolerated with and did not cause a QTc prolongation (40). Data from a chronic toxicity test indicated that oral doses of 40, 80, and 160 mg/kg did not result in any abnormal behavior in mice, with the no-observed-adverse-effect level being 160 mg/kg (41). In addition, the previously reported 50% lethal dose (LD_{50}) of antofloxacin for mice after oral dosing was 1,929 mg/kg (40, 41), which is considerably higher than the maximal dose studied. In this study, the 90% effective dose (ED_{90}) was about 7.5 mg/kg/24 h according to a preliminary survival study (data not shown). At the end of therapy, antofloxacin was observed to produce no toxic effects over the dose range studied up to a dose of 160 mg/kg/24 h, indicating a safety margin (LD_{10}/ED_{90}) of >21.

In conclusion, the bacteriological and bioluminescent evaluations used in our study demonstrated that antofloxacin exhibits dose-dependent *in vivo* activity against *E. coli* in a well-characterized neutropenic murine thigh infection model. The PD index AUC/MIC was a robust predictor of therapeutic efficacy. Both static and killing endpoints were achieved across all study strains, and decreases in the bacterial burden and bioluminescent density were observed at AUC/MIC exposures that exceed the target for stasis of 38.7 h. The PD index and targets identified in this study will be useful for integration with human PK data to optimize the design of clinical dosing regimens for the treatment of uncomplicated urinary tract infection and pyelonephritis with antofloxacin.

MATERIALS AND METHODS

Antimicrobial agent. Antofloxacin hydrochloride (purity, 90.9%) was obtained from the Chinese National Institutes for Food and Drug Control (Beijing, China) as a powder. Test solutions of antofloxacin were freshly prepared prior to the experiments.

Bacterial strains. Eight *E. coli* strains, including seven clinical isolates (isolates 160179, 161406, 161549, 161673, 16X109, 16X327, and 161666) and *E. coli* ATCC 25922, were used in this study (Table 1). Seven clinical *E. coli* strains were isolated from patients with urinary tract infections in the Guangdong Second Traditional Chinese Medicine Hospital. *E. coli* 161549 was transformed with pAK*lux*2 (Addgene plasmid number 14080) (42). This plasmid contains a stable broad-host-range origin of replication enabling plasmid maintenance without antibiotic selection (43, 44). Organisms were grown and subcultured using Mueller-Hinton broth (MHB) and Mueller-Hinton agar (MHA) (Difco Laboratories, Detroit, MI). Bacteria transformed with pAK*lux*2 were cultured in the presence of ampicillin at 60 mg/liter. All *E. coli* isolates were identified by use of a matrix-assisted laser desorption ionization–time of flight mass spectrometry (MALDI-TOF MS) system (Axima Assurance; Shimadzu).

Multiplex PCR was used to detect the presence of seven plasmid-mediated quinolone resistance (PMQR) determinants, i.e., *qnrA*, *qnrB*, *qnrC*, *qnrD*, *qnrS*, *aac(6′)-Ib/cr*, and *qepA*, and PCR amplification of quinolone resistance-determining regions (QRDRs) was carried out as previously described to determine the mutations in the *gyrA* and *parC* genes (45). In addition, the presence of extended spectrum β-lactamase (ESBL) genes (bla_{TEM}, $bla_{CTX\text{-}M}$, and bla_{SHV}) was verified on the basis of PCR testing using our previously described primers (46).

***In vitro* susceptibility.** Antofloxacin MICs were determined using a microdilution method according to the guidelines of the Clinical and Laboratory Standards Institute (CLSI) (47). All MIC tests were

performed in duplicate and on two separate occasions. *E. coli* ATCC 25922 was used as an experimental control.

Murine thigh infection model. The neutropenic murine thigh infection model was used for the *in vivo* study of antofloxacin. Animals were maintained in accordance with the standards of the National Standards for Laboratory Animals of China (GB 14925-2010). All animal studies were approved by the Animal Research Committees of the South China Agriculture University. Six-week-old, specific-pathogen-free, female ICR mice weighing 24 to 27 g (Guangdong Medical Lab Animal Center, Guangzhou, China) were used in this experiment. Neutropenia (neutrophil count, $\leq$100/mm^3) was induced by two doses of cyclophosphamide injected intraperitoneally 4 days (150 mg/kg) and 1 day (100 mg/kg) before experimental infection. An early-logarithmic-phase bacterial suspension (0.1 ml) consisting of approximately 10^6 to 10^7 bacteria was inoculated intramuscularly into each posterior thigh muscle of the mice. Antofloxacin was subcutaneously administered 2 h after thigh infection. After 24 h of treatment, the thighs (four per group) were immediately removed upon euthanasia and homogenized in 3 ml of sterile saline. Each homogenate was serially diluted 10-fold, and 100-μl aliquots of each dilution were plated on MHA plates for counting of the number of CFU of bacteria in each thigh.

This infection model was also used to confirm plasmid stability and for bioluminescent strain characterization, performed by measurement of the bacterial counts in homogenized thigh cultures. Plasmid stability was assessed by comparing the bacterial counts after plating on MHA with and without ampicillin. Bioluminescent strain characterization was done by comparing the bacterial counts of *E. coli* isolates carrying pAK*lux*2 with those of *E. coli* isolates lacking the plasmid.

Drug pharmacokinetics. The single-dose plasma pharmacokinetics of antofloxacin in infected mice were determined following subcutaneous administration of 2.5, 10, 40, and 80 mg/kg. Groups of six mice each were sampled at each time point and dose level. Blood samples were obtained by retro-orbital puncture at the following times after dosing: 0.08, 0.25, 0.5, 0.75, 1, 2, 4, and 8 h. Plasma was isolated by centrifugation of the blood samples at 3,000 $\times$ *g* for 10 min at 4°C. Antofloxacin concentrations in plasma were determined using liquid chromatography-tandem mass spectrometry (LC-MS/MS) as we have described previously (20). The assay limit of quantification (LOQ) and limit of detection (LOD) were 0.01 and 0.005 mg/liter, respectively. The analytical method in plasma was validated by assessing the extraction efficiency and the intra- and interday reproducibility at drug concentrations of 0.01, 0.1, and 1.0 mg/liter. The intraday coefficients of variation for replicate control samples ($n = 5$) varied from 2.1 to 6.2%, and the interday coefficients of variation ranged from 3.5 to 8.7%. The relevant PK parameters, including the elimination half-life ($t_{1/2}$), the area under the concentration-time curve (AUC), the peak (maximum) concentration (C_{max}), and the time of the peak (maximum) concentration (T_{max}), were determined using a one-compartment model with first-order absorption in WinNonlin software (version 6.1; Pharsight, St. Louis, MO, USA). Linear extrapolation was used to estimate the PK parameters for dose levels that were not directly measured in this study. Previous studies have determined that the levels of protein binding of antofloxacin in mice and humans are 20.3% and 17.5%, respectively (12, 20). The free drug fractions were utilized in the PK/PD analyses.

Pharmacodynamic target associated with efficacy. The AUC/MIC ratio was chosen as the predictive PK/PD index correlating with the exposure-response relationships of antofloxacin on the basis of the findings of previous studies (18, 20). *In vivo* treatment experiments were performed using the murine thigh infection model with each isolate of *E. coli*. The dose-response studies included antofloxacin at doses that increased 2-fold from 2.5 to 80 mg/kg and that were administered every 12 h by subcutaneous injection. The dose levels were selected to identify the entire dose-response relationship from maximal to no efficacy. Groups of two mice (four thighs) received each dose regimen. After 24 h of therapy, the mice were euthanized and their thighs were aseptically removed, homogenized, and processed for determination of the number of CFU. Untreated mice received injections of the same volume of sterile saline and were sacrificed at the end of the study period.

The correlation between efficacy and the PK/PD index AUC/MIC was calculated according to a sigmoidal maximum-effect (E_{max}) model derived from the Hill equation (21): $E = (E_{max} \times C^N)/(EC_{50}{}^N + C^N)$, where E is the effector (log change in CFU counts per thigh between treated mice and controls), C is the PK/PD parameter being examined as well as the 24-h total dose, EC_{50} is the value of C required to achieve 50% of E_{max}, and N is the Hill coefficient, which describes the slope of the dose-response curve. These data were analyzed using the nonlinear WinNonlin regression program. The coefficient of determination (R^2) was used to estimate the variance associated with the regression for the PK/PD index. The dosages and 24-h free drug AUC/MIC (fAUC$_{24}$/MIC) targets required to produce a net static effect and 1-log$_{10}$ and 2-log$_{10}$ killing were calculated for each *E. coli* isolate.

***In vivo* bioluminescent monitoring of therapeutic efficacy.** An *in vivo* imaging procedure was developed to provide a noninvasive technique for rapid and real-time monitoring of the therapeutic efficacy of antofloxacin (24). Using the neutropenic murine thigh infection model, mice were infected intramuscularly with an *E. coli* strain containing pAK*lux*2 at 10^6 or 10^8 CFU/thigh. At 2 h postinfection, mice were randomized to receive either (i) the control treatment with the vehicle only or (ii) antofloxacin at 20 mg/kg subcutaneously every 12 h. Mice were anesthetized with 2% isoflurane for bioluminescent imaging with an IVIS Lumina imaging system (PerkinElmer), and the captured bioluminescence data were quantified using Living Image software (version 4.2), provided with the instrument. Images were taken at 2 h after infection and then at 6, 12, 24, and 48 h after treatment. Treatments were monitored for 2 days. Bioluminescent signals were expressed as radiance (in number of photons per second per square centimeter per steradian) using a pseudocolor scale, in which red represents the most intense luminescence and blue represents the least intense luminescence (25). After imaging at the last time point, the control and antofloxacin-treated mice were sacrificed and the bacterial burdens were quantitatively

measured by determination of viable plate counts of whole-thigh homogenates (number of CFU per thigh).

SUPPLEMENTAL MATERIAL

Supplemental material for this article may be found at https://doi.org/10.1128/AAC.01281-17.

SUPPLEMENTAL FILE 1, PDF file, 0.1 MB.

ACKNOWLEDGMENTS

We thank the Guangdong Second Traditional Chinese Medicine Hospital for providing clinical *E. coli* isolates and Attila Karsi for the gift of pAK*lux*2. We acknowledge Rui-Shi Yang for technical assistance.

No conflict of interest with the submission of the manuscript exists, and the manuscript was approved by all authors.

This work was supported by the National Key Research and Development Program of China (2016YFD0501300), the Natural Science Foundation of Guangdong Province (S2012030006590), and the Graduate Student Overseas Study Program of South China Agricultural University (2017LHPY027).

REFERENCES

1. Czaja CA, Scholes D, Hooton TM, Stamm WE. 2007. Population-based epidemiologic analysis of acute pyelonephritis. Clin Infect Dis 45:273–280. https://doi.org/10.1086/519268.
2. Foxman B, Klemstine KL, Brown PD. 2003. Acute pyelonephritis in US hospitals in 1997: hospitalization and in-hospital mortality. Ann Epidemiol 13:144–150. https://doi.org/10.1016/S1047-2797(02)00272-7.
3. Brown P, Ki M, Foxman B. 2005. Acute pyelonephritis among adults: cost of illness and considerations for the economic evaluation of therapy. Pharmacoeconomics 23:1123–1142. https://doi.org/10.2165/00019053-200523110-00005.
4. Scholes D, Hooton TM, Roberts PL, Gupta K, Stapleton AE, Stamm WE. 2005. Risk factors associated with acute pyelonephritis in healthy women. Ann Intern Med 142:20–27. https://doi.org/10.7326/0003-4819-142-1-200501040-00008.
5. Fihn SD. 2003. Clinical practice. Acute uncomplicated urinary tract infection in women. N Engl J Med 349:259–266.
6. Ronald A. 2002. The etiology of urinary tract infection: traditional and emerging pathogens. Am J Med 113(Suppl 1A):14S–19S.
7. Gupta K, Hooton TM, Naber KG, Wullt B, Colgan R, Miller LG, Moran GJ, Nicolle LE, Raz R, Schaeffer AJ, Soper DE. 2011. International clinical practice guidelines for the treatment of acute uncomplicated cystitis and pyelonephritis in women: a 2010 update by the Infectious Diseases Society of America and the European Society for Microbiology and Infectious Diseases. Clin Infect Dis 52:e103–e120. https://doi.org/10.1093/cid/ciq257.
8. Khoshnood S, Heidary M, Mirnejad R, Bahramian A, Sedighi M, Mirzaei H. 2017. Drug-resistant gram-negative uropathogens: a review. Biomed Pharmacother 94:982–994. https://doi.org/10.1016/j.biopha.2017.08.006.
9. Zhang YY, Huang HH, Ren ZY, Zheng HG, Yu YS, Lu XJ, Xiao ZK, Yang HF, Xiu QY, Chen BY, Yue HM, Hao QL, Huang JA, Ma H, Xiao W, Guo DY, Si B, Sun SH, Zhang W, Li QH, Shen HH, Duan J, Li HY, Yao WZ, Gu JM, Xia QM, Ying KJ, Liu A, Yang HP, Shi MH, Sun TY, Ding GH, Wu GM. 2009. Clinical evaluation of oral levofloxacin 500 mg once-daily dosage for treatment of lower respiratory tract infections and urinary tract infections: a prospective multicenter study in China. J Infect Chemother 15:301–311. https://doi.org/10.1007/s10156-009-0713-9.
10. Jeon JH, Kim K, Han WD, Song SH, Park KU, Rhee JE, Song KH, Park WB, Kim ES, Park SW, Kim NJ, Oh MD, Kim HB. 2012. Empirical use of ciprofloxacin for acute uncomplicated pyelonephritis caused by *Escherichia coli* in communities where the prevalence of fluoroquinolone resistance is high. Antimicrob Agents Chemother 56:3043–3046. https://doi.org/10.1128/AAC.06212-11.
11. Ambrose PG, Bhavnani SM, Rubino CM, Louie A, Gumbo T, Forrest A, Drusano GL. 2007. Pharmacokinetics-pharmacodynamics of antimicrobial therapy: it's not just for mice anymore. Clin Infect Dis 44:79–86. https://doi.org/10.1086/510079.
12. Liu L, Pan X, Liu HY, Liu XD, Yang HW, Xie L, Cheng JL, Fan HW, Xiao DW. 2011. Modulation of pharmacokinetics of theophylline by antofloxacin, a novel 8-amino-fluoroquinolone, in humans. Acta Pharmacol Sin 32:1285–1293. https://doi.org/10.1038/aps.2011.78.
13. Ma Y, Wang Q, Zhang H, Xie L, Chen J, Huang M, Liu Y, Wang Y, Wang L, Sun L, Ou N. 2017. Simultaneous quantification of antofloxacin and its major metabolite in human urine by HPLC-MS/MS, and its application to a pharmacokinetic study. Biomed Chromatogr 31:3962. https://doi.org/10.1002/bmc.3962.
14. Xiao Y, Lu Y, Kang Z, Zhang M, Liu Y, Zhang M, Li T. 2008. Pharmacokinetics of antofloxacin hydrochloride, a new fluoroquinolone antibiotic, after single oral dose administration in Chinese healthy male volunteers. Biopharm Drug Dispos 29:167–172. https://doi.org/10.1002/bdd.600.
15. Wagenlehner FM, Kinzig-Schippers M, Tischmeyer U, Wagenlehner C, Sorgel F, Dalhoff A, Naber KG. 2006. Pharmacokinetics of ciprofloxacin XR (1000 mg) versus levofloxacin (500 mg) in plasma and urine of male and female healthy volunteers receiving a single oral dose. Int J Antimicrob Agents 27:7–14.
16. Peloquin CA, Hadad DJ, Molino LP, Palaci M, Boom WH, Dietze R, Johnson JL. 2008. Population pharmacokinetics of levofloxacin, gatifloxacin, and moxifloxacin in adults with pulmonary tuberculosis. Antimicrob Agents Chemother 52:852–857. https://doi.org/10.1128/AAC.01036-07.
17. Wang J, Xiao Y, Huang W, Xu N, Bai C, Xiu Q, Mei C, Zheng Q. 2010. A phase II study of antofloxacin hydrochloride, a novel fluoroquinolone, for the treatment of acute bacterial infections. Chemotherapy 56:378–385. https://doi.org/10.1159/000317581.
18. Xiao XM, Xiao YH. 2008. Pharmacokinetics/pharmacodynamics of antofloxacin hydrochloride in a neutropenic murine thigh model of *Staphylococcus aureus* infection. Acta Pharmacol Sin 29:1253–1260. https://doi.org/10.1111/j.1745-7254.2008.00872.x.
19. Yu X, Wang G, Chen S, Wei G, Shang Y, Dong L, Schon T, Moradigaravand D, Parkhill J, Peacock SJ, Koser CU, Huang H. 2016. Wild-type and non-wild-type *Mycobacterium tuberculosis* MIC distributions for the novel fluoroquinolone antofloxacin compared with those for ofloxacin, levofloxacin, and moxifloxacin. Antimicrob Agents Chemother 60:5232–5237. https://doi.org/10.1128/AAC.00393-16.
20. Zhou YF, Tao MT, Huo W, Liao XP, Sun J, Liu YH. 2017. *In vivo* pharmacokinetic and pharmacodynamic profiles of antofloxacin against *Klebsiella pneumoniae* in a neutropenic murine lung infection model. Antimicrob Agents Chemother 61:e02691-16. https://doi.org/10.1128/AAC.02691-16.
21. Lepak AJ, Andes DR. 2016. *In vivo* pharmacodynamic target assessment of delafloxacin against *Staphylococcus aureus*, *Streptococcus pneumoniae*, and *Klebsiella pneumoniae* in a murine lung infection model. Antimicrob Agents Chemother 60:4764–4769. https://doi.org/10.1128/AAC.00647-16.
22. Andes D, Craig WA. 2002. Pharmacodynamics of the new fluoroquin-

olone gatifloxacin in murine thigh and lung infection models. Antimicrob Agents Chemother 46:1665–1670. https://doi.org/10.1128/AAC.46.6.1665-1670.2002.
23. Zhanel GG, Ennis K, Vercaigne L, Walkty A, Gin AS, Embil J, Smith H, Hoban DJ. 2002. A critical review of the fluoroquinolones: focus on respiratory infections. Drugs 62:13–59. https://doi.org/10.2165/00003495-200262010-00002.
24. Rocchetta HL, Boylan CJ, Foley JW, Iversen PW, LeTourneau DL, McMillian CL, Contag PR, Jenkins DE, Parr TR, Jr. 2001. Validation of a noninvasive, real-time imaging technology using bioluminescent *Escherichia coli* in the neutropenic mouse thigh model of infection. Antimicrob Agents Chemother 45:129–137. https://doi.org/10.1128/AAC.45.1.129-137.2001.
25. Bayer AS, Abdelhady W, Li L, Gonzales R, Xiong YQ. 2016. Comparative efficacies of tedizolid phosphate, linezolid, and vancomycin in a murine model of subcutaneous catheter-related biofilm infection due to methicillin-susceptible and -resistant *Staphylococcus aureus*. Antimicrob Agents Chemother 60:5092–5096. https://doi.org/10.1128/AAC.00880-16.
26. Francis KP, Yu J, Bellinger-Kawahara C, Joh D, Hawkinson MJ, Xiao G, Purchio TF, Caparon MG, Lipsitch M, Contag PR. 2001. Visualizing pneumococcal infections in the lungs of live mice using bioluminescent *Streptococcus pneumoniae* transformed with a novel gram-positive *lux* transposon. Infect Immun 69:3350–3358. https://doi.org/10.1128/IAI.69.5.3350-3358.2001.
27. Brand AM, Smith R, de Kwaadsteniet M, Dicks LM. 2011. Development of a murine model with optimal routes for bacterial infection and treatment, as determined with bioluminescent imaging in C57BL/6 mice. Probiotics Antimicrob Proteins 3:125–131. https://doi.org/10.1007/s12602-011-9069-4.
28. Xiong YQ, Willard J, Kadurugamuwa JL, Yu J, Francis KP, Bayer AS. 2005. Real-time in vivo bioluminescent imaging for evaluating the efficacy of antibiotics in a rat *Staphylococcus aureus* endocarditis model. Antimicrob Agents Chemother 49:380–387. https://doi.org/10.1128/AAC.49.1.380-387.2005.
29. Fodah RA, Scott JB, Tam HH, Yan P, Pfeffer TL, Bundschuh R, Warawa JM. 2014. Correlation of *Klebsiella pneumoniae* comparative genetic analyses with virulence profiles in a murine respiratory disease model. PLoS One 9:e107394. https://doi.org/10.1371/journal.pone.0107394.
30. Rattanaumpawan P, Nachamkin I, Bilker WB, Roy JA, Metlay JP, Zaoutis TE, Lautenbach E. 2017. High fluoroquinolone MIC is associated with fluoroquinolone treatment failure in urinary tract infections caused by fluoroquinolone susceptible *Escherichia coli*. Ann Clin Microbiol Antimicrob 16:25. https://doi.org/10.1186/s12941-017-0202-4.
31. Hooton TM, Winter C, Tiu F, Stamm WE. 1995. Randomized comparative trial and cost analysis of 3-day antimicrobial regimens for treatment of acute cystitis in women. JAMA 273:41–45.
32. Talan DA, Stamm WE, Hooton TM, Moran GJ, Burke T, Iravani A, Reuning-Scherer J, Church DA. 2000. Comparison of ciprofloxacin (7 days) and trimethoprim-sulfamethoxazole (14 days) for acute uncomplicated pyelonephritis in women: a randomized trial. JAMA 283:1583–1590. https://doi.org/10.1001/jama.283.12.1583.
33. Craig WA. 1998. Pharmacokinetic/pharmacodynamic parameters: rationale for antibacterial dosing of mice and men. Clin Infect Dis 26:1–10. https://doi.org/10.1086/516284.
34. Li YF, Wang K, Yin F, He YC, Huang JH, Zheng QS. 2012. Dose findings of antofloxacin hydrochloride for treating bacterial infections in an early clinical trial using PK-PD parameters in healthy volunteers. Acta Pharmacol Sin 33:1424–1430. https://doi.org/10.1038/aps.2012.68.
35. Andes D, Craig WA. 2003. Pharmacodynamics of the new des-f(6)-quinolone garenoxacin in a murine thigh infection model. Antimicrob Agents Chemother 47:3935–3941. https://doi.org/10.1128/AAC.47.12.3935-3941.2003.
36. Lepak AJ, Seiler P, Surivet JP, Ritz D, Kohl C, Andes DR. 2016. *In vivo* pharmacodynamic target investigation of two bacterial topoisomerase inhibitors, ACT-387042 and ACT-292706, in the neutropenic murine thigh model against *Streptococcus pneumoniae* and *Staphylococcus aureus*. Antimicrob Agents Chemother 60:3626–3632. https://doi.org/10.1128/AAC.00363-16.
37. Nayar AS, Dougherty TJ, Reck F, Thresher J, Gao N, Shapiro AB, Ehmann DE. 2015. Target-based resistance in *Pseudomonas aeruginosa* and *Escherichia coli* to NBTI 5463, a novel bacterial type II topoisomerase inhibitor. Antimicrob Agents Chemother 59:331–337. https://doi.org/10.1128/AAC.04077-14.
38. Dougherty TJ, Nayar A, Newman JV, Hopkins S, Stone GG, Johnstone M, Shapiro AB, Cronin M, Reck F, Ehmann DE. 2014. NBTI 5463 is a novel bacterial type II topoisomerase inhibitor with activity against gram-negative bacteria and *in vivo* efficacy. Antimicrob Agents Chemother 58:2657–2664. https://doi.org/10.1128/AAC.02778-13.
39. Stahlmann R. 2002. Clinical toxicological aspects of fluoroquinolones. Toxicol Lett 127:269–277. https://doi.org/10.1016/S0378-4274(01)00509-4.
40. Lv Y, Xiao YH, Liu Y, Xia YH, Li TY. 2008. Tolerance of antofloxacin hydrochloride after ascending single oral dose administration in healthy male volunteers. Chin J Clin Pharmacol 24:17–20.
41. Mei YJ. 2010. Antofloxacin: a novel effective broad-spectrum antimicrobial agent. Anhui Med Pharm J 14:229–231. (In Chinese.)
42. Karsi A, Lawrence ML. 2007. Broad host range fluorescence and bioluminescence expression vectors for Gram-negative bacteria. Plasmid 57:286–295. https://doi.org/10.1016/j.plasmid.2006.11.002.
43. Kovach ME, Elzer PH, Hill DS, Robertson GT, Farris MA, Roop RM, II, Peterson KM. 1995. Four new derivatives of the broad-host-range cloning vector pBBR1MCS, carrying different antibiotic-resistance cassettes. Gene 166:175–176. https://doi.org/10.1016/0378-1119(95)00584-1.
44. Antoine R, Locht C. 1992. Isolation and molecular characterization of a novel broad-host-range plasmid from *Bordetella bronchiseptica* with sequence similarities to plasmids from gram-positive organisms. Mol Microbiol 6:1785–1799. https://doi.org/10.1111/j.1365-2958.1992.tb01351.x.
45. Kim HB, Park CH, Kim CJ, Kim EC, Jacoby GA, Hooper DC. 2009. Prevalence of plasmid-mediated quinolone resistance determinants over a 9-year period. Antimicrob Agents Chemother 53:639–645. https://doi.org/10.1128/AAC.01051-08.
46. Liao XP, Xia J, Yang L, Li L, Sun J, Liu YH, Jiang HX. 2015. Characterization of CTX-M-14-producing *Escherichia coli* from food-producing animals. Front Microbiol 6:1136. https://doi.org/10.3389/fmicb.2015.01136.
47. Clinical and Laboratory Standards Institute. 2015. Performance standards for antimicrobial susceptibility testing; 25th informational supplement. CLSI document M100-S25. Clinical and Laboratory Standards Institute, Wayne, PA.